GEOPHYSICS, VOL. 71, NO. 4 (JULY-AUGUST 2006); P. F49–F60, 6 FIGS., 2 TABLES.
10.1190/1.2216930

Permeability prediction from MICP and NMR data using an electrokinetic approach

P. W. J. Glover[1], I. I. Zadjali[2], and K. A. Frew[3]

ABSTRACT

The accurate modeling of oil, gas, and water reservoirs depends fundamentally upon access to reliable rock permeabilities that cannot be obtained directly from downhole logs. Instead, a range of empirical models are usually employed. We propose a new model that has been derived analytically from electrokinetic theory and is equally valid for all lithologies. The predictions of the new model and four other common models (Kozeny-Carman, Berg, Swanson, and van Baaren) have been compared using measurements carried out on fused and unfused glass bead packs as well as on 91 rock samples representing 11 lithologies and three coring directions. The new model provides the best predictions for the glass bead packs as well for all the lithologies. The crux of the new model is to have a good knowledge of the relevant mean grain diameter, for example, from MICP data. Hence, we have also predicted the permeabilities of 21 North Sea well cores using all five models and five different measures of relevant grain size. These data show that the best predictions are provided by the use of the new model with the geometric mean grain size. We have also applied the new model to the prediction of permeability from NMR data of a 500 m thick sand-shale succession in the North Sea by inverting the T_2 spectrum to provide a value for the geometric mean grain size. The new model shows a good match to all 348 core measurements from the succession, performing better than the SDR, Timur-Coates, HSCM, and Kozeny-Carman predictions.

INTRODUCTION

Permeability is the key reservoir parameter in any reservoir assessment because it controls the accessibility of hydrocarbon accumulations that are present at depth. However, it is an extremely difficult parameter to obtain. Most permeability assessments are carried out on cores, where the permeability of a rock is inferred from pressure and flow rate data. However, cores are not always available. Furthermore, the measurements are expensive, suffer from sampling and experimental uncertainties, and are carried out at a scale that is not representative of the gross fluid flow in the reservoir.

Clearly, it is in our interest to obtain a reliable method for predicting permeability from downhole measurements. No downhole measurement can access permeability directly. However, several techniques have been used to infer permeability from downhole tools. These include (1) poroperm crossplots (Tiab and Donaldson, 1996), (2) principal component analysis (Lee and Datta-Gupta, 1999), (3) cloud transforms (Al Qassab et al., 2000), (4) fuzzy logic (Cuddy and Glover, 2002), (5) neural networks (Helle et al., 2001), (6) genetic algorithms (Cuddy and Glover, 2002), and (7) a range of empirically determined laws that vary in their validity from formation to formation (e.g., Berg, 1970). All of these methods rely on mathematical pattern recognition, a simplifying assumption, or calibration to a data set from a different formation in a different field which is often not even the same lithology.

It is beyond the scope of this paper to consider the first six techniques. There are many types of empirical or semiempirical relationships that are currently used by industry and in university research. Perhaps the one most commonly used is a modified form of the Kozeny-Carman model (Kozeny, 1927; Carman, 1937, 1938, 1956). There are many other models (e.g., Berg, 1970; Van Baaren, 1979; Swanson, 1981; Wyllie and Rose, 1950; Timur, 1968; Morris and Biggs, 1967; Coates and Dumanoir, 1974). Most of these equations use some measure of the diameter of the grain size or of the pore size as well as the porosity of the porous medium. Although the porosity is easy to obtain from a range of downhole tools, until recently, the grain size was not.

The NMR tool is often feted as having the ability to provide downhole permeability measurements directly. However, this claim is

Manuscript received by the Editor July 21, 2005; revised manuscript received December 19, 2005; published online July 11, 2006.
[1]Département de géologie et de génie géologique, Faculté de sciences et de génie, Université Laval, Sainte-Foy, Québec, G1K 7P4, Canada. E-mail: paglover@ggl.ulaval.ca.
[2]Petroleum development Oman, P.O. Box 125, 166, Mina Al Fahal, Muscat, Oman. E-mail: Ibrahim.I.Zadjali@pdo.co.om.
[3]Schlumberger Information Solutions, 5599 San Felipe, Suite 1700, Houston, Texas 77095. E-mail: kfrew@slb.com.

misleading. The current method for obtaining permeability from NMR data is based upon the so-called Timur-Coates equation (Coates et al., 1991). This equation is simply another empirically derived relationship that links various NMR-derived parameters to permeability. However, the NMR tool has the potential of providing the distribution of grain sizes or pore sizes within the rock by inverting the T_2 relaxation time spectrum. These data are expected to be extremely useful (1) because it allows the empirical methods cited above to provide predicted permeabilities using solely downhole data, and (2) the full distribution of grain or pore sizes should allow us to ascertain the most apposite mean grain size to use. It should be said that the method for obtaining grain size from the T_2 relaxation time is an empirical procedure, which may introduce errors into permeability predictions based upon such grain sizes whether the prediction equations are empirically derived themselves or not, as in the case of the RGPZ equation. However, it is expected that better quality predictions should be provided by methods that minimize the use of empirical relationships.

Here we introduce a new permeability prediction equation. Unlike some of the other equations, it does not depend upon calibration to an empirical data set. Instead, it is derived from the consideration of the electrokinetic link between fluid flow and electrical flow that occurs in a porous medium. The method was originally described in an unpublished discussion paper by André Revil, Paul Glover, Philippe Pezard, and M. Zamora. Consequently, we call the new model the RGPZ model. The derivation of the RGPZ model is given in Appendix A.

This paper has two goals: (1) to validate the RGPZ model and to compare its results with those from other common permeability prediction models and (2) to ascertain the optimal method for obtaining the relevant mean grain size from either MICP (laboratory) or NMR (downhole) data.

PERMEABILITY MODELS

We have used a number of permeability prediction tools in this paper. Each will be described briefly in this section. Nelson (1994) suitably divided these methods into those based upon (1) surface area (e.g., Coates et al., 1991), (2) pore size (e.g., Carman, 1938; Swanson, 1981) and (3) grain size (e.g., Berg, 1970; Van Baaren, 1979).

The basic permeability prediction model used with NMR data is the so-called SDR model (Schlumberger Doll Research) (Hidajat et al., 2004). The predicting equation is

$$k_{\mathrm{SDR}} = 4 \times 10^{-11} \phi^4 T_{2lm}^2, \tag{1}$$

where k_{SDR} is in m^2, ϕ is the fractional NMR derived porosity, and T_{2lm} is the logarithmic mean value of the NMR T_2 relaxation time in seconds.

Coates et al. (1991) developed the free fluid model which estimates the permeability based on the free fluid index (FFI,) i.e., the fraction of the rock representing freely moveable water in the porous media, and the bulk volume irreducible (BVI) i.e., the fraction of the rock representing the bound water. The predicting equation is

$$k_{\mathrm{NMR}} \cong 10^{-11} \phi^4 \left(\frac{\mathrm{FFI}}{\mathrm{BVI}} \right)^2, \tag{2}$$

where k_{NMR} is in m^2 and FFI + BVI = ϕ. For a given T_2 distribution, the relative values of FFI and BVI are defined by a threshold [$T_{2\mathrm{cutoff}}$ (in ms)]. In the absence of the laboratory data, 33 and 92 ms are the commonly used $T_{2\mathrm{cutoff}}$ values for sandstones and carbonates, respectively.

More recently, Hidajat et al. (2002) have produced a correlation between fluid permeability and the logarithmic mean T_{2lm} from NMR data. The predicting equation is

$$k_{\mathrm{HSCM}} = \frac{A \rho^2 T_{2lm}^2}{F} = A \rho^2 T_{2lm}^2 \phi^m, \tag{3}$$

where k_{HSCM} is in m^2 and A is a constant determined to be 0.002 by calibration against simulated exponentially correlated 3D porous media. The surface relaxivity $\rho = 2.12 \times 10^{-5}$ m/s after Huang (1997), and T_{2lm} is the logarithmic mean value of the NMR T_2 relaxation time in seconds.

Although all of the NMR-based models are easy to apply, each contains a calibration constant that is valid only for rocks broadly similar to those upon which the calibration was made. It is true that a recalibration may be made for a specific field, but that loses the prediction advantage. However, these models can provide a fairly good initial range of predicted permeabilities directly from downhole NMR data, providing that the NMR data have been analyzed correctly.

The Kozeny-Carmen model (Kozeny, 1927; Carman, 1937; 1938; 1956) derives from the work of Kozeny in 1927 which was subsequently described and reworked by Carman. The form of the model has evolved, but its present form is

$$k_{\mathrm{KC}} = \frac{1}{2 S_{gr}^2} \cdot \frac{\phi^3}{(1 - \phi)^2}, \tag{4}$$

where k_{KC} is in m^2, S_{gr} is the specific surface area of the rock (i.e., internal surface area per grain volume in /m), which is dependent upon the grain shape, d is the median grain size (m), and ϕ is the porosity (fractional). For spherical grains $S_{gr} = 6/d$, and, consequently,

$$k_{KC} = \frac{1}{72} \frac{d^2 \phi^3}{(1 - \phi)^2}. \tag{5}$$

The Swanson (1981) model is an empirical relationship that was created from mercury injection capillary pressure (MICP) data from over 300 cleaned sandstone and carbonate samples from 74 formations. The predicted permeability is given by

$$k_S = 339 \left(\frac{S_{\mathrm{Hg}}}{P} \right)_{\mathrm{apex}}^{1.691}, \tag{6}$$

where k_S is in m^2, and (S_{Hg}/P) is the value of the mercury saturation divided by the applied pressure that corresponds to the apex of the graph of (S_{Hg}/P) as a function of pressure P. The advantage of the Swanson model is that it can provide permeability predictions directly from a single mercury porosimetry measurement. Despite being restricted by its calibration, the range of formations represented by its 300 calibration samples allows its valid application to be fairly wide. It cannot, however, be used on downhole data.

Berg examined grain packing, grain size, grain sorting, and porosity to derive a complex relationship (Berg, 1970), which he subsequently simplified (Berg, 1975) to give

$$k_B = 8.4 \times 10^{-2} d^2 \phi^{5.1}, \tag{7}$$

where k_B is in m^2, d is the grain size (m), and ϕ is the porosity (fractional). The Berg model is finding increasing favor in the industry

because it is simple and often provides fairly good permeability predictions using only two parameters. However, like the other empirical models, good predictions rely on whether it is applied to rocks sharing broadly similar properties to those upon which the equation was calibrated.

The Van Baaren model (Van Baaren, 1979), although derived from the Kozeny-Carmen model, bears a striking similarity to that of Berg (1975). In his review, Nelson (1994) points out that the Van Baaren model is more flexible than the Berg model because it contains two additional variables. It is debatable whether this can be seen as an advantage if it is the robust prediction of permeability that is the ultimate goal. The Van Baaren model is given by

$$k_{VB} = 10 d_d^2 \phi^{(3.64+m)} B^{-3.64}, \tag{8}$$

where k_{VB} is in m^2, d_d is the dominant modal grain size (m), ϕ is the porosity (fractional), m is the cementation exponent, and B is the sorting index which varies from 0.7 for extremely well sorted grains to unity for poorly sorted grains.

All of these models were derived empirically or have certain simplifying assumptions in their derivation. By comparison, the new (RGPZ) model is derived analytically from considerations of the electrokinetic coupling between fluid flow and electrical flow in a porous medium. It cannot be said to be based upon grain size, but it is certainly highly sensitive to that parameter. Consequently, a large portion of this paper is dedicated to analyzing the best method of providing a mean grain size for the RGPZ model. The derivation of the RGPZ model is given in Appendix A. For the RGPZ model, the permeability is given by

$$K_{RGPZ} = \frac{d^2 \phi^{3m}}{4am^2}, \tag{9}$$

where K_{RGPZ} is in m^2, d is the relevant grain size (geometric mean), ϕ is the porosity, m is the cementation exponent, and a is a parameter that is thought to be equal to 8/3 for three dimensional samples composed of quasi-spherical grains. Figure 1 shows the behavior of the RGPZ model as a function of its major parameters over ranges exceeding those commonly encountered in reservoir rocks. Note that the shape of the poroperm plots, Figure 1a–c, is convex-up as we commonly find for poroperm plots of single lithologies. It is worth noting that the model is highly sensitive to changes in d, ϕ and m but is not sensitive to changes in the packing parameter a. We generally use a constant $a = 8/3$ for spherical particles (Schwartz et al., 1989), which is valid for most sedimentary rocks. For spherical particles, $m = 1.5$ and the RGPZ equation becomes

$$K_{RGPZ} = 4.16 \times 10^{-2} d^2 \phi^{4.5}. \tag{10}$$

For $m = 1.8$, the typical value for sandstones, the RGPZ equation becomes

$$K_{RGPZ} = 2.89 \times 10^{-2} d^2 \phi^{5.4}, \tag{11}$$

which is very similar to the Berg model, equation 8. It is expected

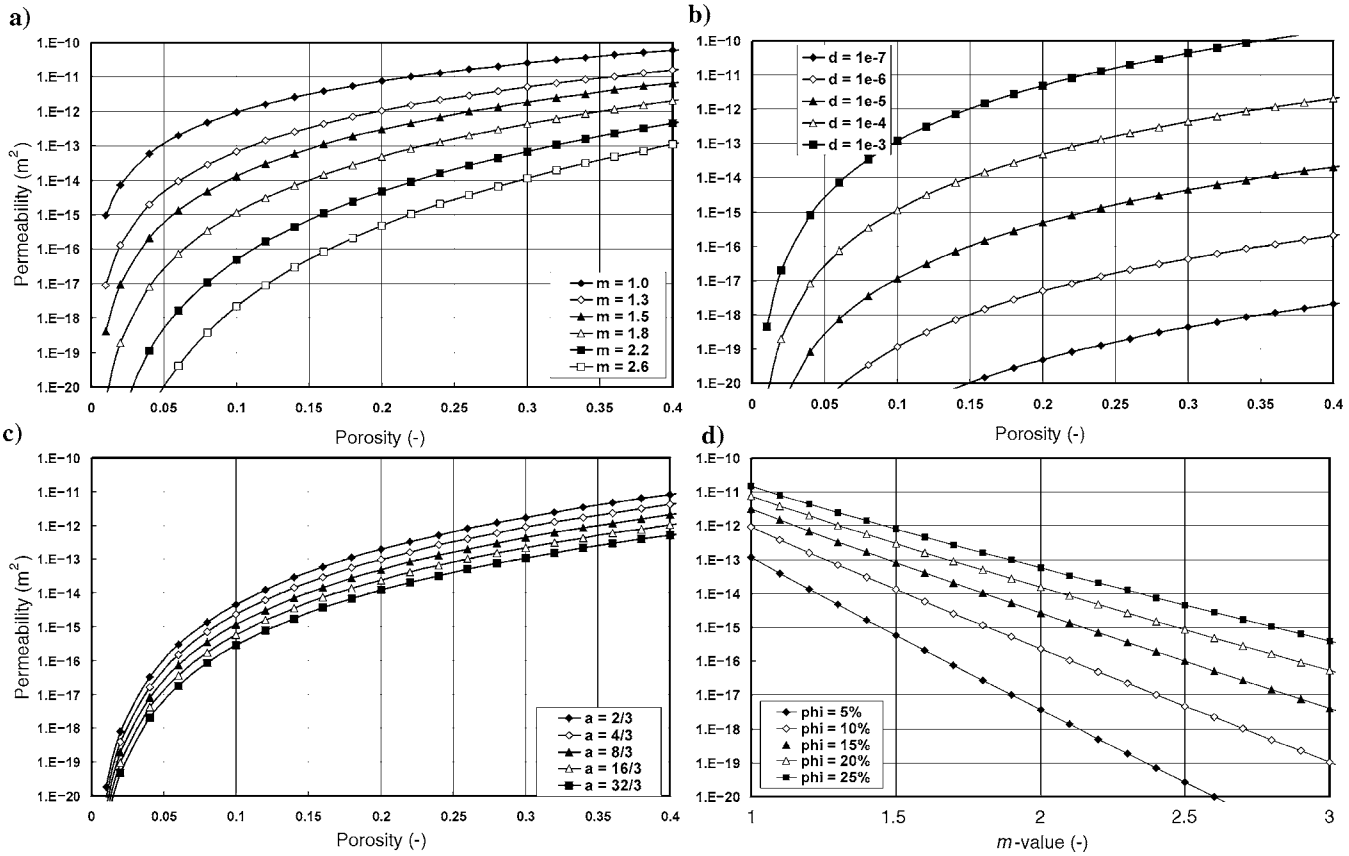

Figure 1. Behavior of the RGPZ model as a function of its major parameters. Predicted permeability as a function of (a) porosity for various values of cementation exponent, (b) porosity for various values of grain size, (c) porosity for various values of the packing parameter, and (d) cementation exponent for various values of porosity.

that the RGPZ model will perform better than the empirical models, especially at low and high permeabilities where the empirical models lack sufficient calibration. It is also expected that the RGPZ equation will exhibit a smaller degree of scattering at all permeabilities because of its greater ability to account for the multivariate behavior of permeability.

VALIDATION OF THE MODEL WITH BEAD PACKS

The RGPZ model has been validated by constructing a set of fluid saturated glass bead packs. The glass beads that were used were soda-lime glass spheres with a high degree of sphericity and a tight tolerance (Endecotts, U. K.). They were randomly packed into a cylindrical cell 2.54 cm in diameter and between 2.5- and 5-cm-long. The samples were saturated with an aqueous solution of 0.1 M NaCl of a known density and electrical resistivity by slow displacement using a Pharmacia P-500 piston pump. Permeabilities were calculated for water flow at five flow rates measured gravimetrically (approximately 0.1, 0.5, 1.0, 4.0, and 8.0 cm^3 per minute, or 1.21, 6.06, 12.12, 48.49, 96.99 barrels/m for a 21.59-cm-diameter production bore): The differential pressure was recorded using a Keithley 2700 digital multimeter and data acquisition system and a high-resolution differential pressure sensor. The porosity was measured using a gravimetric technique. Permeabilities were calculated for each flow rate and no systematic variation of permeability with flow rate was found in this range. Consequently, we have used the arithmetic average of the calculated permeabilities together with their maximum and minimum range as error bars. The complex electrical resistivity of the samples were measured using a Solartron 1260 impedance analyzer and platinum-blacked platinum gauze electrodes from 1 MHz to 0.1 Hz. Measurements were made while no flow was occurring in order to avoid systematic errors due to streaming potentials. The cementation exponent was calculated from the porosity and the modulus resistivity at 1 kHz. The glass bead pack data are shown in Table 1.

Figure 2a shows the predicted and measured permeabilities measured and calculated in this work and from data taken from other authors. The imported data are for glass bead packs, unconsolidated and consolidated sandstones (Chauveteau and Zaitoun, 1981), and for fused glass beads (Johnson et al., 1987). It can be seen that all the experimental data indicate that the RGPZ equation predicts the permeability extremely well over six decades of variation.

Figure 2b shows the measured permeabilities as a function of the grain diameter and compares them with curves representing the RGPZ model and other models. It is clear that the RGPZ and Berg models perform relatively well compared to the modified Kozeny-Carman model or the Van Baaren model. It is also clear that the RGPZ model is the most conservative of the four models tested here.

PERMEABILITY PREDICTION IN ROCKS

The permeability predicted by the RGPZ model and other models has been compared with the measured permeability for 65 samples which represent a range of different lithologies (Table 2). In each case, the permeability was measured using a nitrogen gas permeameter and was corrected, where necessary, for the Klinkenberg and Forscheimer effects. The porosity was measured with a Coberley-Stevens helium pyknometer and by MICP using a Carlo-Erba mercury porosimeter. The formation factor and cementation exponent were measured with QuadTech, Solartron, and Hewlett Packard impedance spectrometers at 1 kHz while the rock was saturated with high salinity aqueous NaCl.

These data have been compiled by the authors over a number of years to allow a broad range of lithologies to be represented. Berea sandstone is a well-known isotropic clean sandstone analog. Darley Dale sandstone is a well-indurated, granular, felspathic quartz with 75% quartz, 15% feldspar (plagioclase and microcline), and 10% muscovite and illite (Glover et al., 1997). It is isotropic, has a moderate porosity (12%–24%), and a high permeability (500–2000 mD or 4.9×10^{-13}–1.97×10^{-12} m^2).

Lochaline sandstone is an extremely pure white sandstone (>99.9% quartz, with 0.04% TiO_2 as the next most dominant oxide by XRF) deposited in the Upper Cretaceous in a depositional environment that has been the subject of much debate. It occurs in an uncemented form and a cemented form, both of which are isotropic. The uncemented form has well-sorted subrounded grains (50–100 μm), has a moderately high porosity (18%–25%) and permeability (500–2000 mD or 4.93×10^{-13}–1.97×10^{-12} m^2), and is mechanically weak enough to be crushed by hand into loose sand. The cemented Lochaline sandstone is chemically identical with the uncemented version except that it has undergone the secondary pre-

Table 1. Data from the glass-bead pack experiments.

	Measured				Predicted			
Bead pack	Grain diameter (μm)	Cementation exponent, m (−)	Porosity, ϕ (−)	Permeability ($\times 10^{-12}$ m^2)	RGPZ permeability ($\times 10^{-12}$ m^2)	Kozeny-Carman permeability ($\times 10^{-12}$ m^2)	Berg permeability ($\times 10^{-12}$ m^2)	Van Baaren permeability ($\times 10^{-12}$ m^2)
A	20	1.49	0.4009	0.2411	0.2695	0.6906	0.3135	1.3180
B	45	1.48	0.3909	1.599	1.3645	3.4962	1.5872	6.6726
C	106	1.50	0.3937	8.118	7.571	19.399	8.80731	37.024
D	250	1.50	0.3982	50.46	42.116	107.908	48.9905	205.946
E	500	1.46	0.3812	186.79	168.465	431.631	195.962	823.784
F	1000	1.47	0.3954	709.85	673.861	1726.52	783.847	3295.14
G	2000	1.49	0.3856	2277.26	2695.44	6906.09	3135.39	13180.5
H	3350	1.48	0.3965	7706.97	7562.40	19375.9	8796.73	36979.7

cipitation of silica on all the original eroded grains. The secondary precipitation is euhedral resulting in very thin planar grain boundaries which represent extremely small pore throats. The euhedral grains interlock and ensure that the rock has a relatively high mechanical strength. The porosity and permeability are consequentially much lower (2%–8% and 1–5 mD or 0.9869×10^{-16}–4.93 $\times 10^{-16}$ m^2). A comparison between the two forms is instructive because of the variation in porosity and permeability derived only from the addition of the secondary quartz overgrowths.

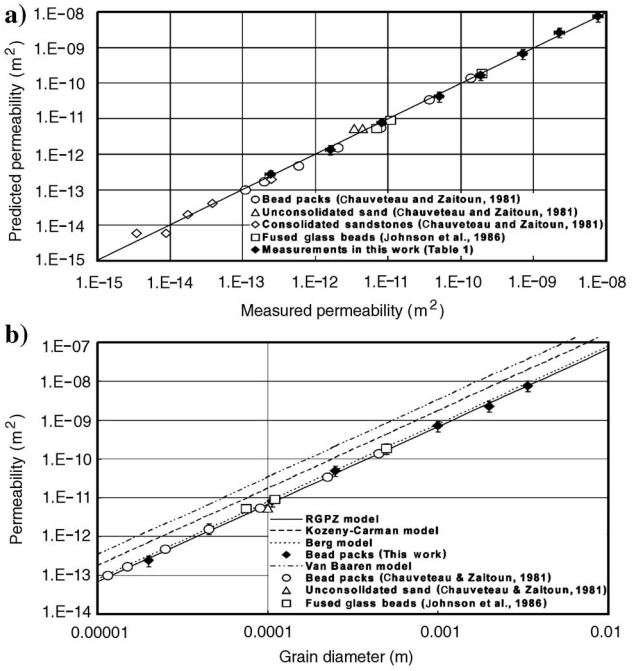

Figure 2. Comparison of the measured and predicted permeabilities for a range of glass bead packs and other data. (a) Predicted permeability using the RGPZ model as a function of measured permeability for soda-lime glass bead packs (Table 1), glass bead packs, unconsolidated sands and consolidated sandstones (Chauveteau and Zaitoun, 1981), and fused glass beads (Johnson et al., 1987). (b) Measured permeability as a function of grain size for soda-lime glass bead packs (Table 1), glass bead packs and unconsolidated sands (Chauveteau and Zaitoun, 1981), and fused glass beads (Johnson et al., 1987) compared with four permeability prediction models (lines: RGPZ, Berg, Kozeny-Carman, and Van Baaren).

Fascally sandstone or siltstone is an upper to middle Jurassic sandstone containing significant amounts of clay minerals with clear bedding. We have cored suites of samples both parallel, perpendicular, and at 45° to the bedding to examine the effect of the bedding on the ability of the models to predict the permeability of the samples. A number of Portland and Purbeck limestones were also tested.

Figure 3 shows the results of predicting the permeability for the lithologies shown in Table 2 using the RGPZ, Kozeny-Carman, and Berg models. Figure 3 also shows the prediction using the apex model of Swanson. It is immediately clear that the RGPZ model is the best of the four models for most of the rock types, especially at high permeabilities, with the data points making a tightly grouped cloud around the one to one line. Most lithologies are well predicted despite variations in porosity, cementation factor, grain size, the presence of secondary overgrowths, and variations in mineralogy. Figure 3a suggests that the capability of the RGPZ model to predict the permeability diminishes for low-permeability rocks; however, the values are still well within what would be considered to be a reasonable range. It should be noted that the measurement of the Fascally sandstone perpendicular to the bedding is systematically overestimated by up to a factor of about five, and there also seems to be a slight overestimation of the Fascally sandstone that was cored at 45° to the bedding plane.

By comparison, the Kozeny-Carman model provides a more diffuse cloud of data points that shows the correct trend at high permeabilities (i.e., proportional to d^2) but overestimates the permeability of all samples by a factor of about 40. The overestimation provided by the Kozeny-Carman model increases at low permeabilities. The Kozeny-Carman model also has the most difficulty predicting the permeability of the Fascally sandstone that was cored and measured perpendicularly to the bedding (overestimations by up to 2000 times). The Berg model produces the correct trend but provides an imprecise prediction that is overestimated by between one and two orders of magnitude. The Berg model also has great difficulty predicting the permeabilities of the Fascally sandstone perpendicular to the bedding, whose permeabilities are overestimated by as much as

Table 2. Data from lithologies used to test the RGPZ model.

Lithology	Bedding	Number of samples	Range of values: Helium porosity (−)	Formation factor (−)	Cementation exponent (−)	Modal grain size (MICP) (μm)	Klinkenberg permeability (m^2 × 10^{-15})
Berea sandstone	Isotropic	20	0.20–0.24	12.6–15.6	1.59–1.90	408–815	1650–7010
Lochaline sandstone	Isotropic, silica cemented	5	0.07–0.08	34.1–78.9	1.40–1.64	43–200	1.75–4.68
Lochaline sandstone	Isotropic, uncemented	3	0.21–0.22	13.8–14.5	1.71–1.74	34–47	1260–1840
Fascally sandstone	Perpendicular	7	0.24–0.28	21.4–26.4	2.13–2.43	30–60	0.0029–0.045
Fascally sandstone	Parallel	6	0.28–0.36	7.1–17.6	1.73–2.30	20–80	1.56–104.3
Fascally sandstone	45° to bedding	6	0.23–0.26	19.4–27.6	2.22–2.33	3–43	0.00588–2.99
Darley Dale sandstone	Isotropic	12	0.16–0.24	17.3–28	1.83–2.06	182–643	40.9–1644
Portland limestone	Perpendicular	2	0.13–0.14	45.8–65.3	1.87–2.12	14–30	0.036–0.090
Purbeck limestone	Isotropic	4	0.04–0.13	35.8–399.7	1.75–1.87	20–40	0.0019–0.49

500 times. The Swanson model performs least well of the three models, providing reasonable, if somewhat imprecise, predictions for the clean sandstones with high permeabilities, but wildly overestimating the permeabilities of all the lower permeability rocks.

Despite the wide variation in their general prediction capabilities, all four of the models seem to have more difficulty predicting the permeability of samples of Fascally sandstone that were cored perpendicular to the bedding compared to those cored parallel or 45° to the bedding. Is there a direction-sensitive parameter in these models that has been misjudged? The parameters used in the models include porosity, grain size, cementation exponent, and the Swanson parameter. The cementation exponent is sensitive to the direction of its measurement, but in this work, it was measured in the relevant direction for each sample. The porosity that was used in the modeling was obtained using a helium method which is not directionally sensitive. The same is true of the Swanson parameter, which is derived from the increasing saturation of mercury within the rock per unit applied pressure resulting from the entry of mercury into the sample on all sides. The grain size is also obtained from the MICP measurements, but it is possible, nevertheless, that these data include a directional bias. The MICP measurements and the calculation of a grain size spectrum themselves are directionally insensitive. However, we have arbitrarily chosen the modal grain size as our measure of the relevant grain size for permeability prediction for the RGPZ, Kozeny-Carman, and Berg models. It may be that this is erroneous, as supported by the following rationalization:

It is known that larger grain sizes provide larger pore sizes between them, and hence produce larger permeabilities. This is despite the fact that some of the large pores will contain smaller grains because the occurrence of large pores filled completely with smaller grains is limited by the dynamic process of preferential grain sedimentation which tends to sort and deposit grains of a similar size and density at any given time. Now imagine a sample of rock that is composed of a volumetric distribution of grains of different sizes with no predefined arrangement of the grains. Suppose that the rock sample is composed of local subvolumes that are composed of one grain size, each of which represents a local permeability. It is the arrangement of these subvolumes that controls the permeability of the sample as a whole. If the subvolumes are arranged in planes parallel to the direction of measurement, the sample's permeability should be calculated by taking the weighted arithmetic mean of the local permeabilities, i.e., using the weighted arithmetic mean of the grain sizes in the permeability prediction equations. If the subvolumes are arranged in planes perpendicular to the direction of measurement, the sample's permeability should be calculated by taking the weighted harmonic mean of the local permeabilities, i.e., using the weighted harmonic mean of the grain sizes. If the subvolumes are arranged randomly, the sample's permeability should be calculated by taking the weighted geometric mean of the local permeabilities, i.e., using the weighted geometric mean of the grain sizes.

However, in Figure 3 the principal modal grain size was used as the relevant grain size for permeability prediction. Because the modal grain size was towards the larger grain size end of the grain size distribution for all the samples studied, the value of the modal grain size was closer to the weighted arithmetic mean of the grain size distribution than to its weighted harmonic mean. This suggests that the modal grain size is not a reliable measure of grain size for the prediction of permeability in rocks because it may be directionally biased,

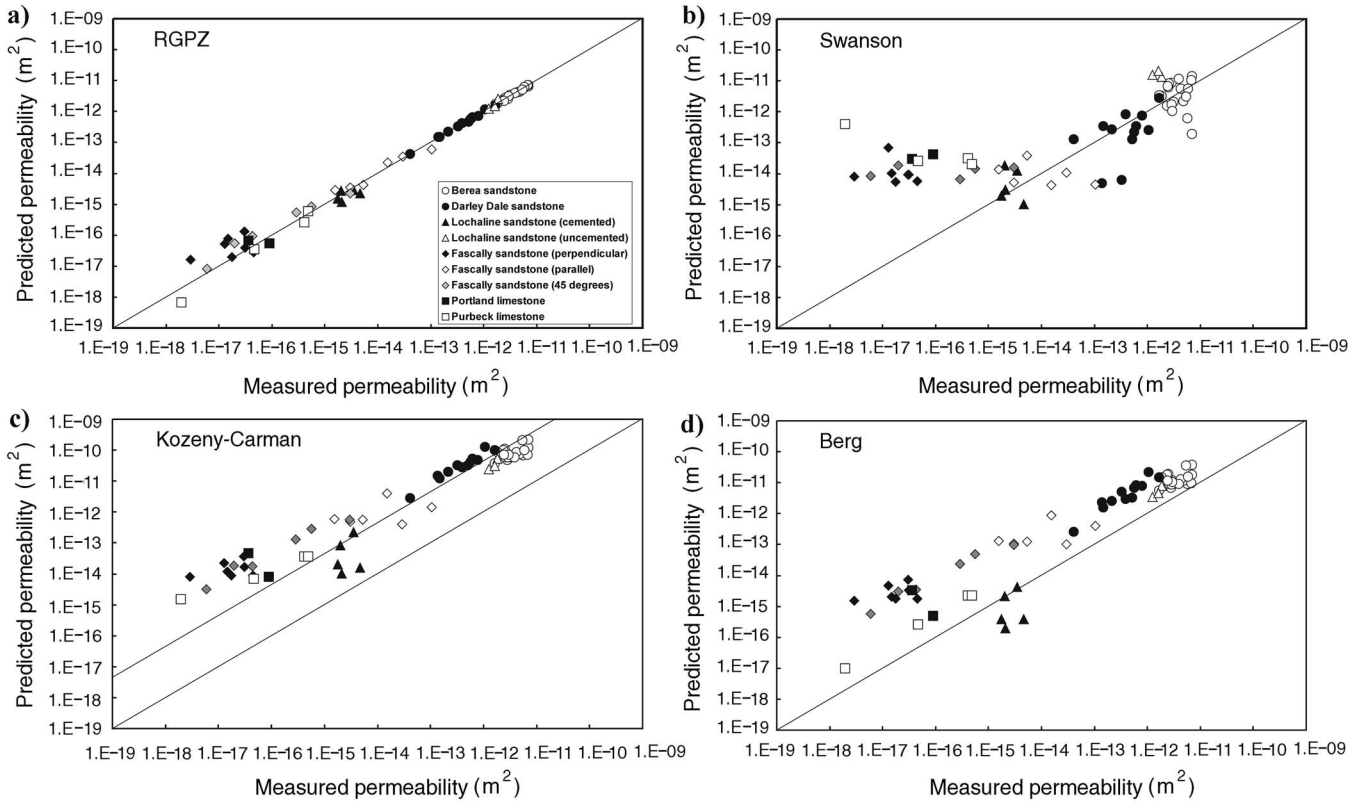

Figure 3. Comparison of the measured and predicted permeabilities for 65 samples of sandstones and carbonates shown in Table 1. (a) RGPZ model, (b) Swanson model, (c) Kozeny-Carman model, and (d) Berg model.

in this case, favoring measurements made parallel to the bedding. One would expect, in Figure 3, that the predicted permeabilities for the Fascally sandstone cored perpendicular to the bedding would be grossly overestimated, as is in fact the case.

To confirm the hypothesis, we calculated the weighted harmonic mean grain sizes for the Fascally perpendicular samples and found that they were approximately seven times smaller than the respective modal grain size. The use of the harmonic mean grain sizes with the RGPZ, Kozeny-Carman, and Berg models results in predicted permeabilities that agree very well with the predicted trend from each model, and in the case of the RGPZ model, provides permeabilities on the 1:1 line.

It is clear that high-quality permeability prediction depends fundamentally on the choice of the relevant mean grain size to use. It was impossible to carry out a more detailed study of this phenomenon with the data set used in Figure 3 because the MICP data was obtained from a porosimeter that lacked sufficient resolution and pressure range. Consequently, we have studied the phenomenon with a high-quality data set obtained from industry in the next section.

PERMEABILITY PREDICTION AND GRAIN SIZE FROM MICP

Real rocks and other naturally derived porous media are composed of a distribution of grain sizes (and shapes). It is not a trivial task to discover the relevant measure of grain diameter for each prediction model. We have used data from 21 cores from an isotropic sandstone succession in the North Sea, U. K. provided by Shell UK Exploration and Production to ascertain the most reliable grain size parameter for permeability prediction. The porosity was measured using a helium porosimeter and the formation factor was measured at 1 kHz using a Hewlett Packard impedance analyzer with the sample saturated with an aqueous solution of 1 M KCl. Grain size spectra were derived from high-quality mercury injection capillary pressure (MICP) measurements made with a Micromeritics mercury porosimeter. In each case, we have confirmed that the results of the grain size distribution are reasonable by comparing them with assessments of the grain size using image analysis of thin sections. Two samples were discarded because the grain size distribution was not consistent with the image analysis assessment. Each grain size spectrum has been analyzed to provide the modal, median, weighted arithmetic mean, weighted geometric mean, and weighted harmonic mean grain size diameters. In several cases, the distribution was multimodal, for which both modal values have been used. The permeability has been predicted with each type of grain size using the RGPZ model and the Kozeny-Carman model. The predicted permeability using the Swanson method has also been calculated. The measured permeability had been obtained by using a nitrogen gas permeameter and had been corrected for the Klinkenberg and Forscheimer effects.

The results from these tests are shown in Figure 4. It is clear that the RGPZ model performs better than the Kozeny-Carman model. It is also clear that the choice of the relevant grain size is extremely important. Figure 4 shows that the median does not provide a relevant or successful measure of grain diameter for use in permeability prediction and may be discarded. For isotropic rocks such as these, the best measures of grain size are the modal grain size (the larger if two peaks are present) and the weighted geometric mean grain size. We hypothesize that the weighted arithmetic mean and weighted harmonic means would be successful at predicting the permeability of clearly bedded rocks, cored parallel and perpendicular to the bedding, based upon the measurements and predictions for the Fascally sandstone. However, further tests on clearly bedded rocks are necessary to confirm this.

While the success of the modal grain size is fairly intuitive, a few words need to be said concerning the weighted geometric mean. It can be shown analytically that the arithmetic and harmonic means represent fluid flow through either a parallel or a series stack of different permeabilities, respectively. By comparison, the geometric mean is thought to represent the permeability of a medium composed of randomly distributed subvolumes of different permeabilities. If we imagine that the distribution of grain sizes within the rock is random and that the permeability of each local volume depends upon the local grain size, it follows that the global permeability may be modeled by using the weighted geometric mean of the grain sizes

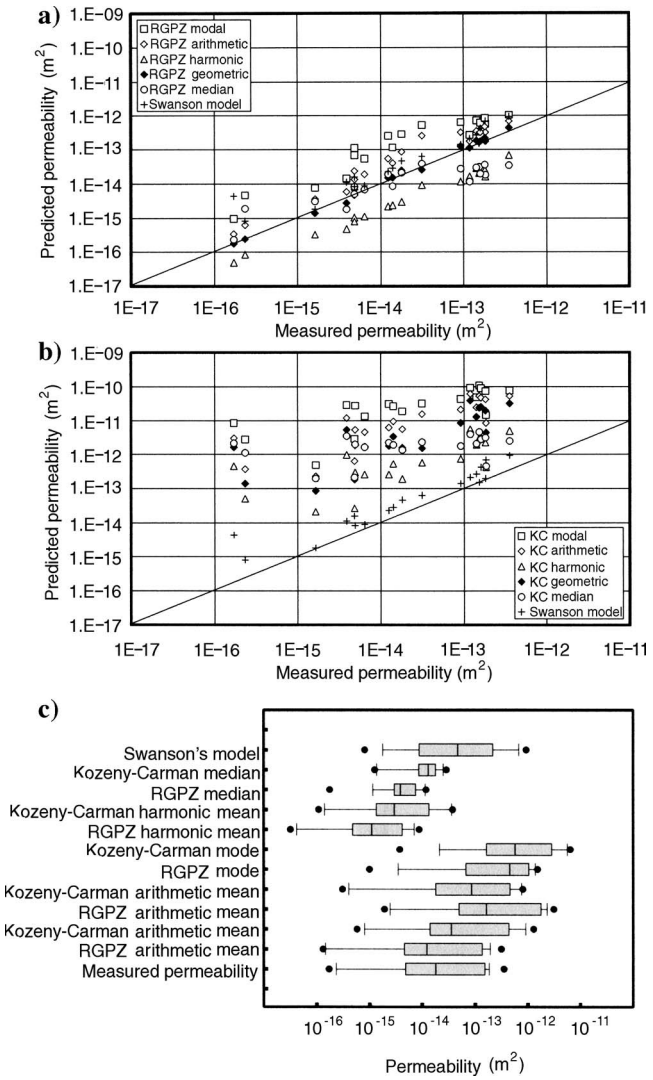

Figure 4. Comparison of the measured and predicted permeabilities for 19 samples of sandstones as a function of five different methods for obtaining the grain size used in the permeability models. (a) RGPZ model with the Swanson model, (b) Kozeny-Carman model with the Swanson model, (c) Predicted and measured permeabilities shown as a box plot (center line is the median, box limits represent 25th to 75th percentiles, whiskers represent 10th and 90th percentiles, dots show extreme points in data).

in the rock. An equivalent approach would be to calculate the permeability for each grain size in the grain size distribution and then to take the weighted geometric mean of the distribution of those permeabilities.

It is interesting to note that the permeability prediction results from the Swanson model, which does not rely on the choice of a grain size measure and performs very well, have been included in Figure 4 for comparison. This is in marked contrast to the results from the previous set of data. We suspect that the Swanson model does provide a high-quality prediction for reservoir sandstones but requires high-quality MICP data for it to work well. The MICP data from the earlier data set were derived from an aging Carlo-Erba porosimeter. The more modern Micromeritics instrument was used to obtain the latter data, which were of much higher quality.

PERMEABILITY PREDICTION AND GRAIN SIZE FROM NMR DATA

The permeability of a 500 m thick succession of sandstones and shales from a well in the North Sea has been predicted using the RGPZ model and four other models. All five models have been compared against permeabilities measured on 348 cores distributed throughout the succession. The data included conventional and Schlumberger MRIL logs and core analysis data. The conventional logs were analyzed to provide porosity, formation factor, and cementation exponent in the conventional way. The MRIL logs were used to calculate the porosity, FFI, BVI and T_{2lm} values. The permeability using the SDR, Coates, and HSCM methods can be calculated directly from these data. In the calculations, we preferred to use the NMR derived porosity because this would always be more convenient for the ultimate user of the NMR log data. The predicted permeabilities from each model are shown in Figure 5 together with the permeability measured on cores.

The RGPZ and Kozeny-Carman models were also used to predict the permeability from this log set. However, both require the input of a relevant grain size. The challenge is to derive such a grain size from the NMR data. We have chosen to adopt a similar approach to that of Basan et al. (1997) and Coates et al. (1999). Initially we derived a representative pore throat size from the NMR data using

$$\Gamma_{\text{throat}} = \frac{\Gamma_{\text{pore}}}{\lambda} = \frac{\rho T_{2lm}}{\lambda}, \tag{12}$$

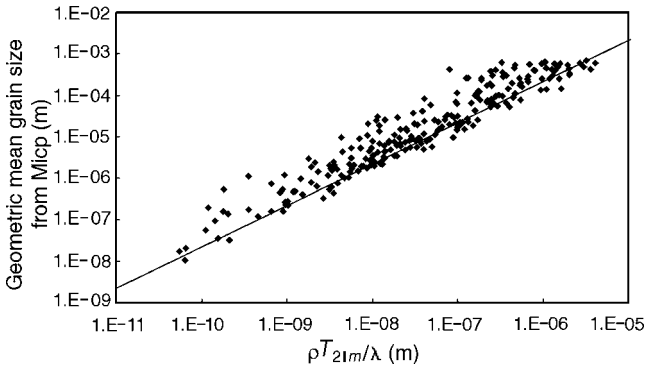

Figure 5. Crossplot of the geometric mean grain size derived from MICP measurements on cores with the value $\rho T_{2lm}/\lambda$ derived from NMR tool data. The line represents the best linear fit, whose gradient is equal to $C = 218.4$.

where Γ_{throat} is a length scale associated with the pore throat diameter (in meters), Γ_{pore} is a length scale associated with the pore diameter (in meters), ρ is the surface reflexivity (in m/s), T_{2lm} is the logarithmic mean value of the NMR T_2 relaxation time (in seconds) and λ is the mean ratio of Γ_{pore} to Γ_{throat}. In this work the value $\lambda = 60$ has been used. This value was obtained from the pore diameters and grain diameters derived from the application of Meyer-Stowe theory to MICP core data from each of the cores taken from the logged section, and has been checked against microphotographs of thin sections from 35 of the 348 cores (10% of the cores). A value of $\rho = 2.12 \times 10^{-5}$ m/s has been used after Huang (1997).

The pore throat diameter thus obtained was correlated with the geometric mean grain size to provide a scaling factor C that was used to convert the pore throat diameter to grain diameter. The calculation of the grain size thus becomes

$$d_{\text{grain}} = C\frac{\rho T_{2lm}}{\lambda} = D\rho T_{2lm}. \tag{13}$$

Figure 5 shows the correlation between grain size and pore throat size for the logged interval. It was found that $C = 218.4 \pm 17.29$, with $R^2 = 0.7022$ by assuming $\lambda = 60$.

It is clear that this method of obtaining grain size is specific to each formation. It requires two initially unknown parameters λ and C, which usually will not be available. Further work is necessary to be able to say whether there is a large natural variation in λ and C, or whether they can be taken to be approximately constant for a range of rock types. However, both depend solely upon the geometry of the pore space. Hence, we have carried out a correlation directly between the product ρT_{2lm} and the geometric mean grain size to provide a single scaling factor D that can be used to convert the product ρT_{2lm} to grain diameter directly (Figure 5). It was found that $D = 3.64 \pm 0.2881$, with $R^2 = 0.7022$.

Figure 6 shows the NMR derived porosities and core derived porosities, together with the core derived permeabilities and the permeability predictions from five models that use the NMR data in their prediction. It is clear from the porosity log that there is a low background porosity ($\phi < 0.03$) with a number of clearly defined high-porosity horizons ($0.1 < \phi < 0.2$). It is reasonable to expect these horizons to have permeabilities that are significantly larger than the background permeability.

The SDR and Coates models predict a background permeability of about 0.01 mD (9.87×10^{-18} m^2) and permeable horizons around 100 mD (9.87×10^{-14} m^2) which overestimates the permeability of most of the permeable horizons by comparison with the permeability measured from the core material. This overestimation can be up to two orders of magnitude. The HSCM model, by comparison, predicts a background permeability of around 0.1 mD (9.87×10^{-17} m^2) and permeable horizons up to 1 mD (9.87×10^{-16} m^2). This represents an underestimation of the permeability of some permeable horizons and a slight overestimation of others. Indeed, the lack of contrast between the background permeability and the predictions for the permeable horizons makes it difficult to distinguish the high-permeability horizons using the HSCM model alone.

The Kozeny-Carman and RGPZ models predict a background permeability of about 0.01 mD (9.87×10^{-18} m^2) and about 0.001 mD (9.87×10^{-19} m^2), respectively. Both models predict the position and the permeability of the permeable horizons very well. However, the Kozeny-Carman model tends to underestimate the

permeability slightly for some permeable horizons, whereas the RGPZ model provides highly accurate permeability predictions for all eight permeable horizons.

LIMITATIONS OF THE RGPZ MODEL

Although the RGPZ model seems to provide good predictions for the experimental and downhole data that we have shown in this work, it is important that its limitations are made clear.

- Although the RGPZ model is not empirical, but derived analytically from electro-kinetic considerations, its application requires knowledge of a characteristic grain size.
- If the RGPZ equation is used with downhole NMR data, the required characteristic grain size currently can be obtained only by employing an empirical procedure relating grain size to the T_2 relaxation time.
- The F and m values used in the equation should be derived from saline water bearing rock to minimize perturbation of the results by surface conduction.
- The value of F should be significantly greater than unity. This constraint means that the RGPZ equation should not be used in low-porosity fractured rocks. However, it should be valid in high-porosity fractured rocks.
- The RGPZ equation is not valid in the limit that $\phi \rightarrow 1$ (i.e., 100% porosity), which amounts to a trivial restriction of the model.
- The RGPZ equation relies on the assumption that O'Konski's equation (O'Konski, 1960) for spherical grains can be used for nonspherical grains providing the grain radius therein is taken as an equivalent or characteristic grain radius. This is valid providing the range of grain radii in the target rock is bigger than the average difference between the smallest radius and the largest radius of each particle. This is true for almost all sedimentary rocks and is described in detail in the Appendix A.

CONCLUSIONS

A new model for the prediction of the fluid permeability of porous media has been proposed. The new model is derived from the consideration of the electrokinetic link between fluid flow and electrical flow in a porous medium. Theoretically, the new (RGPZ) model is valid providing (1) the range of grain sizes in the rock is large compared to the difference between the mean maximum and minimum effective grain radii, (2) the F and m values are derived from saline water bearing rock, (3) the rock is unfractured such that $F \gg 1$, and (4) the model is not used in the limit $\phi \rightarrow 1$ (i.e., 100% porosity). None of these limitations seriously affects its application to many reservoir rocks.

The RGPZ model has been tested with (1) bead pack data (this work), (2) bead pack data from other authors, (3) fused bead pack data from other authors, (4) consolidated and unconsolidated sand data from other authors, (5) 65 samples of various lithologies (this work), (6) 21 samples from a North Sea sandstone succession (this work), and (7) a conventional and NMR logged interval from a well in the North Sea compared against measured permeability of retrieved core (this work). In all cases, the RGPZ model has performed well compared with the true measured permeability and has out-performed seven other common permeability prediction methods (Kozeny-Carman, Swanson, Berg, Van Baaren, Coates, SDR, and HSCM).

The quality of the prediction provided by the RGPZ model (as well as the Kozeny-Carman, Berg, and Van Baaren models) depends critically upon the choice of a relevant weighted mean grain size. It is best to use a weighted geometric mean for isotropic rocks, although the modal grain size also often works well. It is recommended that a weighted harmonic mean of the grain size distribution is used for the permeability prediction of a rock measured perpendicular to a well-developed bedding, and that a weighted arithmetic mean is used for the permeability prediction of a rock measured parallel to a well-developed bedding.

The RGPZ model has been combined with a method to obtain the grain size from NMR log data. The resulting permeability prediction was an excellent match with the retrieved core data, and better than permeability predictions using the Coates equation or the Kozeny-Carman equation. The RGPZ model is clearly an improvement on the other permeability predictors, and could be used to predict permeability if analyzing data from NMR tools.

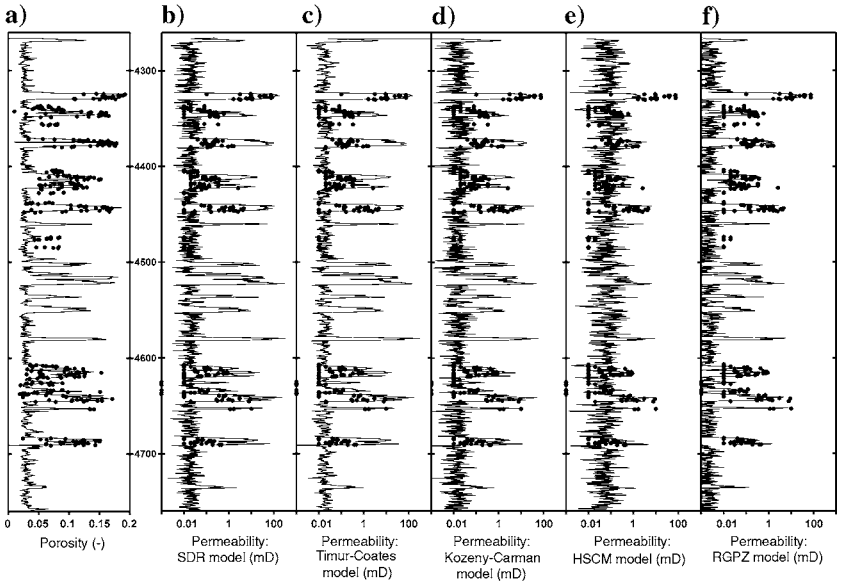

Figure 6. Logs showing the laboratory measured porosity and permeability on cores as filled circles together with log-derived porosity measurements and predicted permeabilities as lines. (a): Laboratory measured core porosity as filled circles and log-derived total porosity as a line. (b)–(f): Laboratory measured core permeability as filled circles with predicted permeabilities using the SDR, Timur-Coates, Kozeny-Carman, HSCM, and RGPZ models shown as lines.

ACKNOWLEDGMENTS

The author would like to thank André Revil, Philippe Pezard, and Maria Zamora who contributed to early work on the RGPZ model. The author would also like to thank the anonymous donor of the MRIL data and MICP data sets. The

comments of two anonymous reviewers helped to improve the paper considerably.

APPENDIX A
THE DERIVATION OF THE RGPZ EQUATION

The Bruggeman-Hanai-Sen (BHS) equation resulted from using the self-consistent medium theory to model the dielectric and conductive responses of a composite porous medium composed of two constituents (Bruggeman, 1935; Hanai, 1960; 1961). The same result has also been obtained by Sen et al. (1981) using a differential effective medium approach. The BHS equation can be written as

$$\frac{\sigma - \sigma_m}{\sigma_f - \sigma_m}\left(\frac{\sigma_f}{\sigma}\right)^D = \phi, \tag{A-1}$$

where ϕ is the interconnected porosity of the porous rock, σ is the macroscopic electrical conductivity of the porous rock, σ_m is the electrical conductivity of the mineral grains including that of the associated surface diffuse layer, and σ_f is the electrical conductivity of the pore fluid. The parameter D is called the depolarization factor and depends strongly on the topology of the interconnected pore space and the shape of the grains (Sen et al., 1981). For a low-density dispersion of spherical grains in a conductive fluid $D = 1/3$ (Bruggeman, 1935), but it has been shown that D retains this value if the spheres form a denser porous medium (Sen et al., 1981). Mendelson and Cohen (1982) have shown that $0 \leq D \leq 1$ whatever the topology of the pore space, and Sherman (1985) has obtained $0.32 \leq D \leq 0.38$ for sandstone from laboratory dielectric measurements. However, for the purposes of this derivation, we allow D to vary.

The BHS equation does not implicitly account for the presence of surface conduction, which is necessary if the equation is to be applied to porous media containing clay minerals. However, the effect of coating nonconducting grains with a specific surface conductivity Σ_s is exactly equivalent to assigning to the grains a total matrix conductivity of

$$\sigma_m = \frac{2\Sigma_s}{R}, \tag{A-2}$$

where R is the radius of the grains (O'Konski, 1960). Hence, the surface conductivity σ_s is also $\sigma_s = 2\Sigma_s/R$. It should be noted that this transform is only strictly valid for spherical grains. For nonspherical grains (e.g., ellipsoids, rods, and disks), O'Konski (1960) gives other, more complex, expressions. However, for the purposes of this derivation, we will assume that $\sigma_s = 2\Sigma_s/R$ remains valid to a first approximation providing we take R as the equivalent grain radius.

The above assumption is valid providing that the grains are close to spherical compared to the range of grain sizes in the rock. We can state the restriction more quantitatively as follows: The aspect ratio of a grain can be defined as $\alpha = d_{max}/d_{min}$, where d_{max} is the largest diameter of the grain and d_{min} is its smallest diameter. The weighted arithmetic mean of an ensemble of such grains with different aspect ratios α and a mean effective grain diameter D_{mean} can be assigned the symbol $\langle \alpha \rangle$. If D_{min} is the effective diameter of the smallest grain in the ensemble and D_{max} is that of the largest grain in the ensemble, we can define their difference $\Delta D = D_{max} - D_{min}$ to be the range of grain sizes in the ensemble. Now it is possible to state the condition that $\langle \alpha \rangle D_{mean} \ll \Delta D$. If this condition is true, the assumption is valid. The condition is true for almost all clastic rocks and for all bead packs. For example, a typical reservoir sandstone with subrounded grains where $\langle \alpha \rangle = 2$, $D_{mean} = 100$ μm, and $\Delta D = 990$ μm would fulfill the condition. However, an atypical clastic rock composed of well-sorted elongated grains with $\langle \alpha \rangle = 5$, $D_{mean} = 100$ μm, and $\Delta D = 300$ μm would fail the condition. In the case of bead packs of a single grain size, the range of grain sizes is fairly small if high quality glass beads are used. However, their sphericity is also extremely good, $\langle \alpha \rangle \rightarrow 1$, and hence the O'Konski equation is valid without needing to make any assumptions.

Following Bussian (1983), we define $m \equiv 1/(1 - D)$, and rewrite the BHS equation, equation A-1 as

$$\sigma = \sigma_f \phi^m \left(\frac{1 - \sigma_s/\sigma_f}{1 - \sigma_s/\sigma}\right)^m. \tag{A-3}$$

Because $0 \leq D \leq 1$, it follows that $m \leq 1$. Hence, equation A-3 can be rewritten as

$$\frac{\sigma}{\sigma_f} = \phi^{m/(1-m)} \left(\frac{1 - \sigma_f/\sigma_s}{1 - \sigma/\sigma_s}\right)^{m/(1-m)}. \tag{A-4}$$

The inverse of the classical formation factor F, and the low-salinity formation factor f are given by the limits of the ratio of rock conductivity to fluid conductivity (i.e., equation A-4) in the limit as the surface conductivity goes to zero and to infinity, respectively. By taking these limits with equation, A-4 we obtain

$$\frac{1}{F} = \lim_{\sigma_s \rightarrow 0}\left(\frac{\sigma}{\sigma_f}\right) = \phi^m, \tag{A-5}$$

and

$$\frac{1}{f} = \lim_{\sigma_s \rightarrow \infty}\left(\frac{\sigma}{\sigma_f}\right) = \phi^{m/(1-m)}. \tag{A-6}$$

It is clear that the parameter m, defined above as $m = 1/(1 - D)$, is identical to the Archie cementation exponent because equation A-5 is Archie's law (Archie, 1942), as theoretically justified by Sen et al. (1981) and Mendelson and Cohen (1982) for granular porous media. Note that for the special case of $m = 2$, we have $f = 1/F$.

The cementation exponent is a measure of the decoupling between the porosity, which is a purely geometric parameter, and the effective part of this porosity used by the electrical current during the electromigration of ions. If the interconnected pore space is formed by a network of interconnected open fractures, it can be shown analytically that $F = 1/\phi$, i.e., $m = 1$, and consequently, all the porosity contributes effectively to the total conductivity. This is not the case for clay-bearing rocks, where high-cementation exponents ($m > 2.5$) indicate that a large fraction of the pore space (microporosity) does not contribute effectively to conduction due to dead-end pores and highly tortuous current paths.

We now define a nondimensional parameter

$$\xi \equiv \frac{\sigma_s}{\sigma_f} = \frac{2\Sigma_s}{R\sigma_f}, \tag{A-7}$$

i.e., ξ is the ratio of the surface conductivity to the free electrolyte conductivity. As noted by Kan and Sen (1987), this is a key parameter allowing the variation of electrical conductivity with salinity to be mapped ($\xi \gg 1$ for the low-salinity domain, and $0 < \xi < 1$ for the high-salinity domain). In the high-salinity domain equation A-3 can be simplified by using the binomial expansion (Bussian, 1983)

$$\sigma = \frac{1}{F}(\sigma_f + m(F-1)\sigma_s). \quad \text{(A-8)}$$

This equation is similar to the linearized equation obtained by Sen (1987) for the electrical conductivity of a 3D periodic array of charged spheres in an electrolyte. In the high-salinity limit, the electrical conductivity is also given by Johnson and Sen (1988) as

$$\sigma = \frac{1}{F}\left(\sigma_f + \frac{2}{\Lambda}\Sigma_s\right), \quad \text{(A-9)}$$

where Λ is the length scale that is the characteristic pore-size dimension associated with transport in the interconnected pore space volume (Johnson and Sen, 1988; Pride, 1994). The parameter Λ can be interpreted as an effective pore radius for transport in the porous medium. The parameter Λ is not rigorously a geometrical parameter. However, it approximates to the radius of the narrow throats that control transport in the interconnected pore volume (e.g., Schwartz et al., 1989; Bernabé and Revil, 1995).

A comparison of coefficients between equations A-8 and A-9 gives

$$\Lambda = \frac{R}{m(F-1)} \cong \frac{R}{mF} = \frac{d}{2mF}, \quad \text{(A-10)}$$

where d is the representative mean diameter of the grains. The approximation that $F - 1 = F$ is valid if $F \gg 1$, which is reasonable for most porous media. Equation A-10 constitutes a new relationship between the length scale Λ and the formation factor F. For the limit of a dilute concentration of spheres (i.e., $\phi \to 1$) we can expand F as a function of ϕ, which gives $F \approx \phi^{-3/2} = 1 + (3/2)(1-\phi)$, with $m = 3/2$ for perfect spheres according to Sen et al. (1981). So, the length scale Λ in this limit is given by $\Lambda = 4R/(9(1-\phi))$ which as already been established by Kostek et al. (1992) using a different method.

It is known that the length scale is related to the hydraulic permeability through a relationship of the form (e.g., Schwartz et al., 1989; Kostek et al., 1992; and Bernabé and Revil, 1995)

$$k \approx \frac{\Lambda^2}{aF}, \quad \text{(A-11)}$$

where a is a constant in the range 2–12 depending upon the topology of the pore space, and is equal to 8/3 for three-dimensional arrangements of quasi-spherical grains. For a three-dimensional grain consolidation model, Kostek et al. (1992) have shown that equation A-11 gives a very good approximation of the hydraulic permeability except in the limit $\phi \to 1$, where ϕ is the interconnected porosity. Consequently, we can derive the RGPZ equation from equations A-10 and A-11:

$$k_{\mathrm{RGPZ}} \cong \frac{d^2}{4am^2F^3} = \frac{d^2\phi^{3m}}{4am^2} = \frac{3d^2\phi^{3m}}{32m^2}. \quad \text{(A-12)}$$

For spheres, $m = 1.5$, and k_{RGPZ} becomes

$$k_{\mathrm{RGPZ}} \cong \frac{d^2\phi^{3m}}{24}. \quad \text{(A-13)}$$

REFERENCES

Al Qassab H. M., J. Fitzmaurice, Z. A. Al-Ali, M. A. Al-Khalifa, G. A. Aktas, and P. W. J. Glover, 2000, Cross-discipline integration in reservoir modeling: The impact on fluid flow simulation and reservoir management: Annual Technical Conference and Exhibition, SPE, SPE 62902.

Archie, G. E., 1942, The electrical resistivity log as an aid in determining some reservoir characteristics: Transactions of the American Institute of Mechanical Engineers, **146**, 54–67.

Basan, P. B., B. D. Lowden, P. R. Whattler, and J. J. Attard, 1997, Pore-size data in petrophysics: A perspective on the measurement of pore geometry, *in* M. A. Lovell, and P. K. Harvey, eds., Developments in petrophysics: Geological Society of Great Britain Special Publication, **122**, 47–67.

Berg, R. R., 1970, Method for determining permeability from reservoir rock properties: Transactions of the Gulf Coast Association of Geological Societies, **20**, 303–317.

———, 1975, Capillary pressures in stratigraphic traps: AAPG Bulletin, **59**, 929–956.

Bernabé, Y., and A. Revil, 1995, Pore-scale heterogeneity, energy dissipation and the transport properties of rocks: Geophysical Research Letters, **22**, 1529–1532.

Bruggeman, D. A. G., 1935, Berechnung verschiedener physikalischer Konstanten von heterogenen Substanzen: Annales Physik, **24**, 636–664.

Bussian, A. E., 1983, Electrical conductance in a porous medium: Geophysics, **48**, 1258–1268.

Carman, P. C., 1937, Fluid flow through a granular bed: Transactions of the Institution of Chemical Engineers, **15**, 150–167.

———, 1938, The determination of the specific surfaces of powders I: Journal of the Society of the Chemical Industrialists, **57**, 225–234.

———, 1956, Flow of gases through porous media: Butterworths.

Chauveteau, G., and A. Zaitoun, 1981, Basic rheological behavior of xanthan polysaccharide solutions in porous media: Effect of pore size and polymer concentration, *in* F. J. Fayers, ed., Enhanced oil recovery, Elsevier Science Publishing Company, Inc., 197–212.

Coates, G. R., and J. L. Dumanoir, 1974, A new approach to improved log-derived permeability: The Log Analyst, **15**, 17–23.

Coates,G. R. , R. C. A. Peveraro, A. Hardwick, and D. Roberts, 1991, The magnetic resonance imaging log characterized by comparison with petrophysical properties and laboratory core data: Proceedings of the 66th Annual Technical Conference and Exhibition, Formation Evaluation and Reservoir Geology, SPE, SPE 22723, 627–635.

Coates, G. R., L. Xiao, and M. G. Prammer, 1999, NMR well logging, Principles and applications: Halliburton Energy Services.

Cuddy, S. J., and P. W. J. Glover, 2002, The application of fuzzy logic and genetic algorithms to reservoir characterization and modeling, *in* P. M. Wong, F. Aminzadeh, and M. Nikravesh, eds., Soft computing for reservoir characterization and modeling, Studies in fuzziness and soft computing series, 80: Physica-Verlag 219–242.

Glover, P. W. J., J. B. Gomez, P. G. Meredith, K. Hayashi, P. R. Sammonds, and S. A. F. Murrell, 1997, Damage of saturated rocks undergoing triaxial deformation using complex electrical conductivity measurements: Experimental results: Physics and Chemistry of the Earth, **22**, 57–61.

Hanai, T., 1960, Theory of the dielectric dispersion due to the interfacial polarization and its application to emulsions: Kolloid-Zeitschrift, **171**, 23–31.

———, 1961, Dielectric on the interfacial polarization for two-phase mixtures: Bulletin of the Institute of Chemical Research of Kyoto University, **39**, 341–367.

Helle, H. B., A. Bhatt, and B. Ursin, 2001, Porosity and permeability prediction from wireline logs using artificial neural networks: A North Sea case study: Geophysical Prospecting, **49**, 431–444.

Hidajat, I., K. K. Mohanty, M. Flaum, and G. J. Hirasaki, 2004, Study of vuggy carbonates using NMR and X-Ray CT scanning: Society of Petroleum Engineers Reservoir Evaluation and Engineering, **7**, 365–377.

Hidajat, I., M. Singh, J. Cooper, and K. K. Mohanty, 2002, Permeability of porous media from simulated NMR response: Transport in Porous Media, **48**, 225–247.

Huang, C. C., 1997, Estimation of rock properties by NMR relaxation methods: M.S. thesis, Rice University.

Johnson, D. L., T. J. Plona, and H. Kojima, 1987, Probing porous media with 1st sound, 2nd sound, 4th sound and 3rd sound, *in* J. R. Banavar, and K. W. Winkler, eds., Physics and chemistry of porous media II: American Institute of Physics Conference Proceedings, 154, 243–277.

Johnson, D. L., and P. N. Sen, 1988, Dependence of the conductivity of a porous medium on electrolyte conductivity: Physics Review B, **37**, 3502–3510.

Kan, R., and P. N. Sen, 1987, Electrolytic conduction in periodic arrays of insulators with charges: Journal of Chemical Physics, **86**, 5748–5756.

Kostek, S., L. M. Schwartz, and D. L. Johnson, 1992, Fluid permeability in porous media, Comparison of electrical estimates with hydrodynamical calculations: Physics Review B, **45**, 186–195.

Kozeny, J., 1927, Über Kapillare Leitung des Wassers im Boden (Aufsteig Versikeung und Anwendung auf die Bemasserung): Math-Naturwissenschaften, **136**, 271–306.
Lee, S. H., and A. Datta-Gupta, 1999, Electrofacies characterization and permeability predictions in carbonate reservoirs: Role of multivariate analysis and nonparametric regression: Annual Technical Conference and Exhibition, SPE, SPE 56658.
Mendelson, K. S., and M. H. Cohen, 1982, The effects of grain anisotropy on the electrical properties of sedimentary rocks: Geophysics, **47**, 257–263.
Morris, R. L., and W.-P. Biggs, 1967, Using log-derived values of water saturation and porosity: Transactions of the 8th Annual Logging Symposium, Society of Petrophysicists and Well Log Analysts, Paper X.
Nelson, P. H., 1994, Permeability-porosity relationships in sedimentary rocks: The Log Analyst, **3**, 38–62.
O'Konski, C. T., 1960, Electric properties of macromolecules, V: Theory of ionic polarization in polyelectrolytes: Journal of Chemical Physics, **64**, 605–619.
Pride, S., 1994, Governing equations for the coupled electro-magnetics and acoustics of porous media: Physics Review B, **50**, 15678–15696.
Schwartz, L. M., P. N. Sen, and D. L. Johnson, 1989, Influence of rough surfaces on electrolytic conduction in porous media: Physics Review B, **40**, 2450–2458.
Sen, P. N., 1987, Electrolytic conduction past arrays of charged insulating spheres: Journal of Chemical Physics, **87**, 4100–4107.
Sen, P. N., C. Scala, and M. H. Cohen, 1981, Self-similar model for sedimentary rocks with application to the dielectric constant of fused glass beads: Geophysics, **46**, 781–795.
Sherman, M., 1985, The calculation of porosity from dielectric constant measurements: A study using laboratory data: Transactions of the 26th Annual Logging Symposium, Society of Petrophysicists and Well Log Analysts, Paper HH.
Swanson, B. F., 1981, A simple correlation between permeabilities and mercury capillary pressures: Journal of Petroleum Technology, **33**, 2498–2504.
Tiab, D., and E. C. Donaldson, 1996, Petrophysics: Theory and practice of measuring reservoir rock and fluid transport properties: Gulf Publishing Company.
Timur, A., 1968, An investigation of permeability, porosity and residual water saturation relationships for sandstone reservoirs: The Log Analyst, **9**, 8–17.
Van Baaren, J. P., 1979, Quick-look permeability estimates using sidewall samples and porosity logs: Transactions of the 6th Annual European Logging Symposium, Society of Petrophysicists and Well Log Analysts, 19–25.
Wyllie, M. R. J., and W. D. Rose, 1950, Some theoretical considerations related to the quantitative evaluation of the physical characteristics of reservoir rock from electric log data: Transactions of the American Institute of Mechanical Engineers, **189**, 105–118.